

FIRST FLIGHT RESULT OF ATTITUDE DETERMINATION FOR 50KG CLASS MICRO SATELLITE SDS-4

Naomi Murakami⁽¹⁾, Yuta Nakajima⁽²⁾, Takashi Ohtani⁽³⁾, Yosuke Nakamura⁽⁴⁾,
Koichi Inoue⁽⁵⁾, and Keiichi Hirako⁽⁶⁾

⁽¹⁾⁻⁽⁶⁾ Japan Aerospace Exploration Agency, 2-1-1, Tsukuba, Ibaraki, 305-8505, Japan,
+81-50-3362-3725, murakami.naomi@jaxa.jp

Abstract: *Small Demonstration Satellite 4 (SDS-4) is the first zero momentum three-axis controlled micro satellite from Japan Aerospace eXploration Agency (JAXA). It was launched on May 17, 2012, and is now operating successfully. For 50 kg-class micro satellites like SDS-4, size limitation is a common problem, which restricts the layouts of ACS components. As to SDS-4, the difficulty is that there can be mounted only one star tracker due to size restrictions. Although SDS-4 has a star tracker for precise attitude determination, it is not always able to track stars because the satellite's nominal attitude is defined inertially-fixed. To optimize the attitude determination accuracy, SDS-4 implements an algebraic attitude estimation using sun and magnetic field sensors, which is used as an alternative to the star tracker measurement. This paper presents an approach for precise attitude determination in 50 kg-class micro satellites, including its ground test process, and introduces the first flight results and current understanding of the in-orbit operation over the past 5 months.*

Keywords: *micro satellite, attitude determination, flight result*

1. Introduction

JAXA Space Technology Demonstration Research Center (STDRC) runs a Small Demonstration Satellite (SDS) program, which provides compact and low-cost standard satellite platforms to demonstrate newly developed components and advanced space technologies. The SDS program also helps nurture the capacity of young engineers through in-house work, exploiting a short development cycle from conceptual design to launch and operation. The first satellite from the SDS program was SDS-1, which was a 100 kg-class spin-stabilized micro satellite launched in 2009. It was inherited from our former satellite, MicroLabSat, which was a 50 kg-class spin-stabilized micro satellite launched in 2002. In response to increasing demands from various missions, such as Earth observation or science, SDS-4, the first three-axis stabilized micro satellite from the SDS program was initiated in 2009.

2. Platform Design

2.1. Small Demonstration Satellite 4 (SDS-4)

On May 17, 2012, SDS-4 was launched by an H-IIA launch vehicle into a sun-synchronous orbit at an altitude of 677 km and local time of the ascending node of 13:30. It was launched as one of the piggyback payloads under the Global Change Observation Mission first Water (GCOM-W1) and the Korean Multi Purpose Satellite 3 (KOMPSAT-3). SDS-4 has four main missions: 1. Space-based Automatic Identification System Experiment (SPAISE), 2. Quartz Crystal Microbalance (QCM), 3. Flat Heat Pipe On-orbit Experiment (FOX) and 4. In-flight Experiment

of Space Materials using Thermal Control Material (IST). The weight and dimensions of SDS-4 are approximately 50 kg and $50 \times 50 \times 45$ cm, respectively, which is the maximum permissible in the given space as a piggyback payload. SDS-4 is controlled in an inertially-fixed sun-oriented attitude at the request of these missions. In addition to these technology demonstration missions, SDS-4 has another important goal, namely to obtain a 50 kg-class precise three-axis controlled bus system for coming advanced missions. Although the required pointing accuracy from missions is 5 deg (3σ), SDS-4 is designed to achieve pointing accuracy of 0.47 deg (3σ) when the star tracker is available, to meet future requirements of upcoming missions. SDS-4 also conducts Earth pointing and target pointing operations as bus experiments. Figure 1 shows the appearance of SDS-4. The satellite's body frame is also illustrated. The reference attitude is defined as follows:

Roll axis (X_b): pointing toward the Sun

Pitch axis (Y_b): along the cross product of the sun and the Earth's north pole vector

Yaw axis (Z_b): in the direction of the Earth's south pole vector, constructed as $X_b \times Y_b$ where suffix b indicates the satellite body frame.

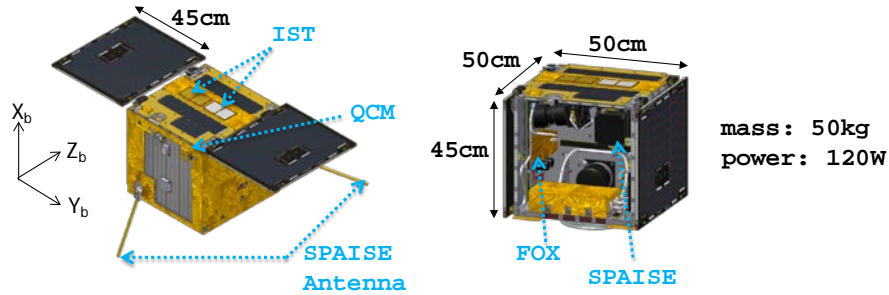


Figure 1. Small Demonstration Satellite 4 (SDS-4)

2.2. Attitude Control Subsystem (ACS)

The SDS-4 ACS is a key subsystem for accomplishing the 50 kg-class precise three-axis controlled satellite platform. Figure 2 shows the ACS components and their layouts, which are packed into a small space. During the component selection process, we prioritized their sizes as well as performance. We have also newly developed a three-axis rate sensor using MEMS vibrating structure gyros to achieve the required performance in a more compact form.

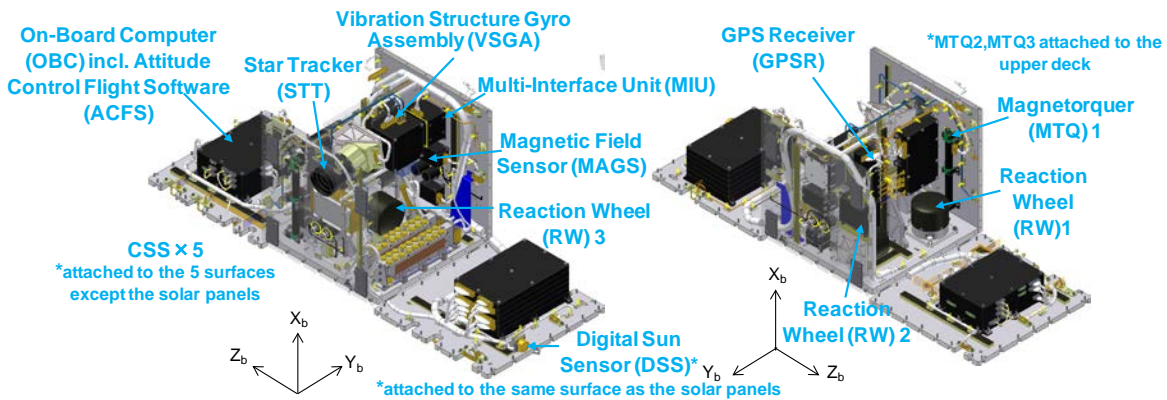


Figure 2. ACS components

SDS-4 adopts zero momentum control with 3 Reaction Wheels (RWs), which provide sufficient control capability. For micro satellites like SDS-4, the key point for achieving high accuracy is how to improve the attitude determination accuracy. SDS-4 uses a Star Tracker (STT) for precise attitude determination. However, the difficulty is that only one STT can be mounted due to size restrictions. Since the satellite attitude is inertially fixed, it is inevitable that reflected sunlight from the Earth will enter into the STT's Earth exclusion angle or the Earth itself will enter into the STT's field of view during a certain period in every orbital pass, resulting in STT unavailability in attitude measurement. To avoid any loss of accuracy during these periods, ACS implements algebraic attitude determination using sun and magnetic field vectors, which is then applied as an alternative to STT measurement.

The ACS hardware and software are integrated to constitute a closed-loop as shown in Fig. 3. The ACS control frequency is 1 Hz and it uses an Extended Kalman Filter for attitude determination, exploiting the rate sensor (VSGA) data for time update and either STT or calculated quaternion data via the QUEST method for measurement update.

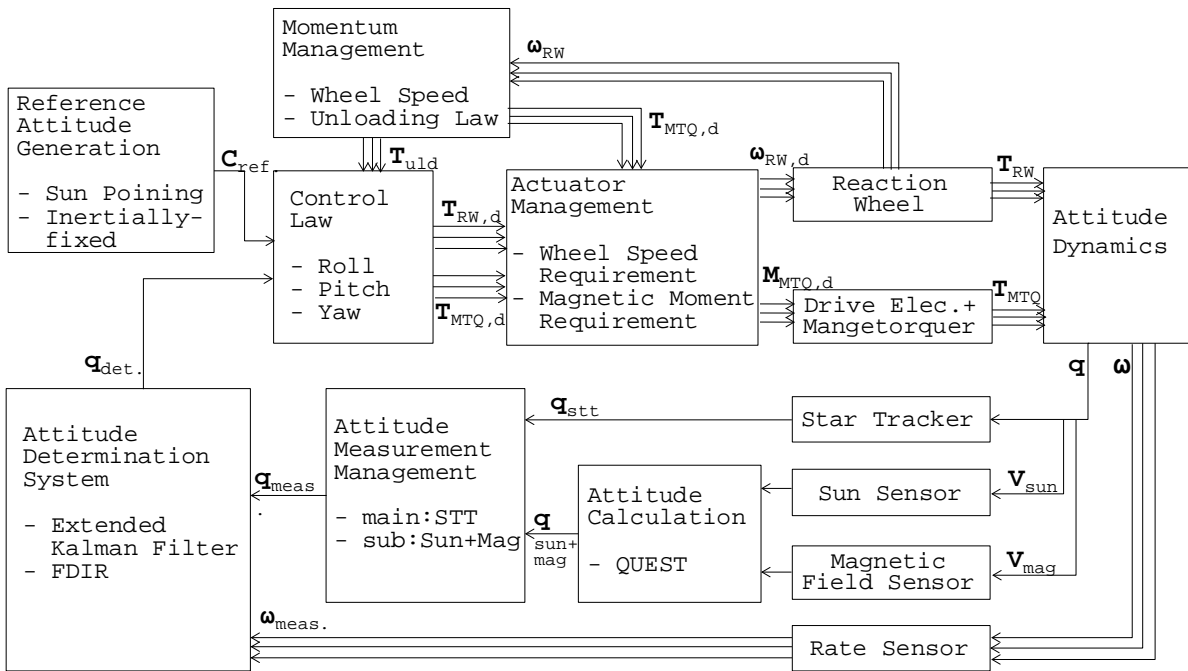


Figure 3. ACS closed-loop block diagram

2.3. Attitude Measurement using Star Tracker (STT)

The SDS-4 STT was selected with emphasis on its size and performance. Table 1 lists the major specification of SDS-4 STT. STT provides attitude quaternions of the satellite's body frame with respect to the J2000.0 inertial frame at a period of 4 Hz. STT is allocated with its boresight in a minus-Yb direction with 10 degrees inclination from the solar panel, which was determined to optimize the period of STT availability. In the preflight analysis, STT unavailability was predicted to start at a latitude of about 20 deg in the ascending pass and end at about 10 deg in the descending pass, as indicated in Fig. 4. The worst duration time was 43 minutes.

Table 1. Specification of Star Tracker

Supplier	Vectronic Aerospace
Data	Attitude quaternion
Field of view	14° × 14°
Measurement error (3σ, total)	Random: 0.052 deg Bias: 0.081 deg (due to possible misalignment)
Exclusion angle	Earth: 35 deg Sun: 40 deg
Mass	850 g
Size	80 × 100 × 180.5 mm

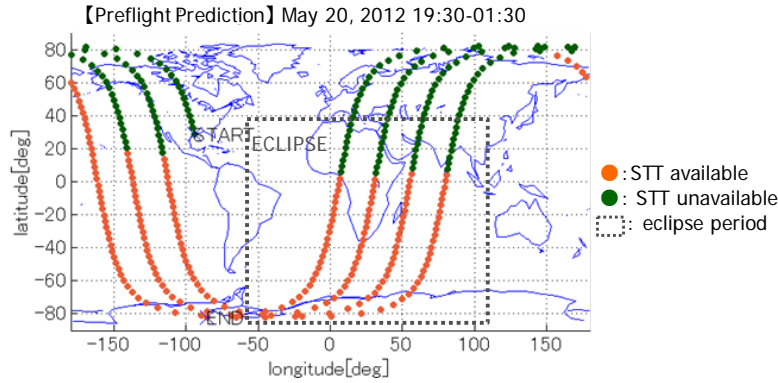


Figure 4. Preflight prediction of STT availability

2.4. Attitude Measurement using the QUEST method

To minimize any impairment in accuracy during the unavailability of STT, ACS implements static attitude estimation using the sun and magnetic field vectors. These vectors in the inertial frame are calculated through the sun location and IGRF-11 geomagnetic field models, respectively. The precise time information required for both is obtained by a GPS Receiver (GPSR), while the position information required for the IGRF model is calculated through an on-board SGP4 orbit propagator. The sun and magnetic field vectors in the body frame are measured using a Digital Sun Sensor (DSS) and Magnetic Field Sensor (MAGS), respectively. It is noted that DSS has a boresight vector attached normal to the solar panels. The two pairs of vectors are used to calculate the inertial-to-body attitude quaternion using the QUEST algorithm. Figure 5 shows a schematic diagram of this process.

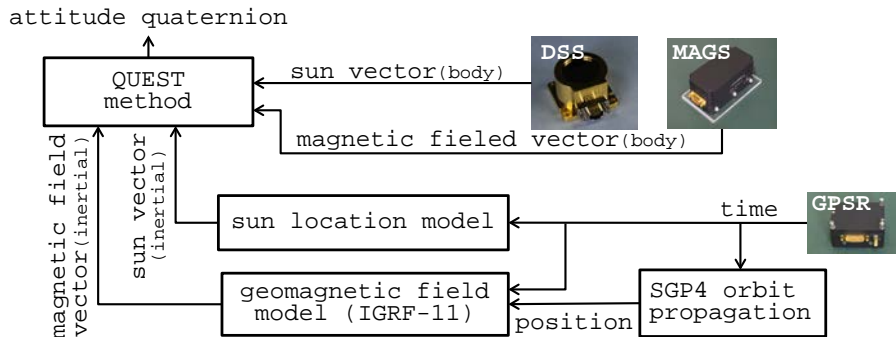


Figure 5. Schematic Diagram of the QUEST attitude measurement

The error from this method depends on the sensor error, model error and the angle between the sun and magnetic field vectors. The sensor random errors are 0.176 deg (1σ) for DSS, and 1.95 deg (1σ) for MAGS, respectively, including measurement delay. It is noted that this MAGS error value is derived from in-orbit evaluation and we assumed it to be 1.19 deg before the launch. The original MAGS accuracy is far better. However, the slight change in RW speed affects the magnetic field around MAGS and impairs accuracy. Though MAGS is located away from RWs as far as possible to minimize this effect, the impact is unavoidable under such crowded component layouts. The error covariance of the QUEST-estimated attitude is calculated via the following equation:

$$\mathbf{P}_{\theta\theta} = \langle \delta\theta \delta\theta^T \rangle = \sigma_{tot}^2 \left[\mathbf{I}_{3 \times 3} - a_{sun} \mathbf{w}_{sun} \mathbf{w}_{sun}^T - a_{mag} \mathbf{w}_{mag} \mathbf{w}_{mag}^T \right]^{-1} \quad (1)$$

$$\sigma_{tot}^2 = \frac{\sigma_{sun}^2 \sigma_{mag}^2}{\sigma_{sun}^2 + \sigma_{mag}^2}, \quad a_{sun} = \frac{\sigma_{mag}^2}{\sigma_{sun}^2 + \sigma_{mag}^2}, \quad a_{mag} = 1 - a_{sun}$$

where $\delta\theta = [\delta\phi, \delta\theta, \delta\psi]^T$, which represents the estimated errors in roll, pitch and yaw axes. \mathbf{w}_{sun} and \mathbf{w}_{mag} are the measured sun and magnetic field vectors in the body frame, respectively. σ_{sun} is 0.177 deg, including the DSS error and the model error of 14 arcsec. σ_{mag} is 1.97 deg including the MAGS error and the IGRF-11 model error of 0.24 deg.

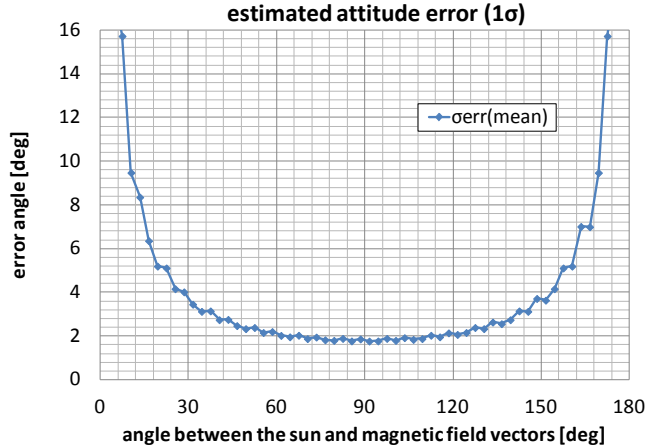


Figure 6. Estimated Attitude Error (1σ) in the QUEST method

Figure 6 indicates the estimated error against the angle between the sun and magnetic field vectors, as obtained from statistical analysis, giving any possible sun and magnetic field vectors. Optimal accuracy of about 2 deg (1σ) is attained when the two vectors are orthogonal, but gets worse as the two vectors become parallel. When the EKF uses the attitude quaternion calculated by the QUEST method, the error covariance is also given as information on the measurement noise. Accordingly, the EKF can avoid any direct decline in accuracy during the period for which both vectors are nearly parallel. In addition, we set a threshold for the valid angular range between both vectors of 45 – 135 deg, and a waiting time of 7 minutes before using the QUEST attitude as an alternative to STT, which values were figured out to optimize the accuracy of the EKF determined attitude. The measurement error of the QUEST method occurs around the measured vectors, especially the sun vector, which contributes significantly to the QUEST method. Since the satellite's roll (Xb) axis is controlled to point towards the sun, the attitude

determination error is mainly attributable to the roll angle when the QUEST attitude is used for the EKF measurement update.

2.5. Vibration Structure Gyro Assembly (VSGA)

SDS-4 has a 3-axis rate sensor called VSGA, which consists of three MEMS vibrating structure gyros and an interface circuit. VSGA provides the integrated satellite's angular rate at 10 Hz. The random drift noise and the random walk drift noise of VSGA are $0.1 \text{ deg/h}^{0.5}$ and $10.25 \text{ deg/h}^{1.5}$, respectively. For further details, see the reference [2].

2.6. Extended Kalman Filter for Attitude Determination

SDS-4 ACS uses the Extended Kalman Filter (EKF) which estimates attitude quaternions $\mathbf{q} = [q_1 \ q_2 \ q_3 \ q_4]^T$ and VSGA rate biases $\mathbf{b} = [b_x \ b_y \ b_z]^T$. Here, attitude quaternions \mathbf{q} are defined to represent the rotation from the Earth's J2000 inertial coordinate frame to the satellite's body frame. The process model describing the attitude kinematics and the sensor dynamics is

$$\dot{\mathbf{q}} = \frac{1}{2} \begin{bmatrix} 0 & \omega_z & -\omega_y & \omega_x \\ -\omega_z & 0 & \omega_x & \omega_y \\ \omega_y & -\omega_x & 0 & \omega_z \\ -\omega_x & -\omega_y & -\omega_z & 0 \end{bmatrix} \mathbf{q} = \frac{1}{2} \Omega(\boldsymbol{\omega}) \mathbf{q} \quad (2)$$

$$\dot{\mathbf{b}} = \boldsymbol{\eta}_2, \quad \boldsymbol{\omega} = \boldsymbol{\omega}_{meas} - \mathbf{b} - \boldsymbol{\eta}_1, \quad \mathbf{Q} = E[\boldsymbol{\eta}\boldsymbol{\eta}^T] \quad (\boldsymbol{\eta} \equiv [\boldsymbol{\eta}_1^T \ \boldsymbol{\eta}_2^T])$$

where a dot over a symbol means the time derivative. $\boldsymbol{\omega} = [\omega_x \ \omega_y \ \omega_z]$ and $\boldsymbol{\omega}_{meas} = [\omega_{x,meas} \ \omega_{y,meas} \ \omega_{z,meas}]$ represents the true satellite's angular rate and VSGA measured angular rate in the body frame, respectively. The VSGA random drift noise is $\boldsymbol{\eta}_1 = [\eta_{1x} \ \eta_{1y} \ \eta_{1z}]^T$, VSGA random walk drift noise is $\boldsymbol{\eta}_2 = [\eta_{2x} \ \eta_{2y} \ \eta_{2z}]^T$, and the covariance matrix of the process noise is \mathbf{Q} . The observation model of the observed quaternion \mathbf{q}_{meas} is given by

$$\mathbf{q}_{v,meas} = \begin{bmatrix} I_{3 \times 3} & 0_{3 \times 3} \end{bmatrix} \begin{bmatrix} \mathbf{q}_v^T \\ \mathbf{b}^T \end{bmatrix} + \mathbf{v}, \quad \mathbf{R} = E[\mathbf{v}\mathbf{v}^T] \quad (3)$$

where \mathbf{v} is a quaternion measurement noise vector, which is defined as $\mathbf{v} = [\sigma q_{1,meas} \ \sigma q_{2,meas} \ \sigma q_{3,meas}]^T$, and \mathbf{R} is a covariance matrix of the quaternion measurement noise. These nonlinear equations are linearized around the steady state \mathbf{q}_{ref} and \mathbf{b}_{ref} , which are defined as follows:

$$\begin{bmatrix} \mathbf{q} \\ \mathbf{b} \end{bmatrix} = \begin{bmatrix} \mathbf{q}_{ref} \ \Delta \mathbf{q} \\ \mathbf{b}_{ref} + \Delta \mathbf{b} \end{bmatrix} \quad (4)$$

where $\Delta \mathbf{q}_v$ and $\Delta \mathbf{b}$ are residual time-varying quantities. Here, $\Delta \mathbf{q}_v$ is defined as $\Delta \mathbf{q}_v = [\Delta q_1 \ \Delta q_2 \ \Delta q_3]^T$. Δq_4 is derived via the equation of $\Delta q_4^2 = 1 - (\Delta q_1^2 + \Delta q_2^2 + \Delta q_3^2)$. Equation 2 is linearized as

$$\begin{bmatrix} \dot{\mathbf{q}}_{ref} \\ \dot{\mathbf{b}}_{ref} \end{bmatrix} = \begin{bmatrix} \frac{1}{2} \Omega(\boldsymbol{\omega}_{ref}) \mathbf{q}_{ref} \\ 0 \end{bmatrix}, \quad \boldsymbol{\omega}_{ref} = \boldsymbol{\omega}_{meas} - \mathbf{b}_{ref} \quad (5)$$

$$\begin{bmatrix} \Delta \dot{\mathbf{q}}_v \\ \Delta \dot{\mathbf{b}} \end{bmatrix} = \begin{bmatrix} \Gamma(\boldsymbol{\omega}_{ref}) & -\frac{1}{2} I_{3 \times 3} \\ 0_{3 \times 3} & 0_{3 \times 3} \end{bmatrix} \cdot \begin{bmatrix} \Delta \mathbf{q}_v \\ \Delta \mathbf{b} \end{bmatrix} + \begin{bmatrix} -\frac{1}{2} I_{3 \times 3} & 0_{3 \times 3} \\ 0_{3 \times 3} & I_{3 \times 3} \end{bmatrix} \cdot \begin{bmatrix} \boldsymbol{\eta}_1 \\ \boldsymbol{\eta}_2 \end{bmatrix}, \quad \Gamma(\boldsymbol{\omega}) = \begin{bmatrix} 0 & \omega_z & -\omega_y \\ -\omega_z & 0 & \omega_x \\ \omega_y & -\omega_x & 0 \end{bmatrix}$$

Equation 3 is also linearized as

$$\mathbf{q}_{v,meas} - \mathbf{q}_{ref} = [I_{3 \times 3} \quad 0_{3 \times 3}] \begin{bmatrix} \Delta \mathbf{q}_v^T \\ \Delta \mathbf{b}^T \end{bmatrix} + \mathbf{v} \quad (6)$$

The EKF formulation is applied to $\Delta \mathbf{q}_v$ and $\Delta \mathbf{b}$ according to the process model shown in Eq. 5 and the observation model shown in Eq. 6. In the SDS-4 EKF, the steady state of \mathbf{q}_{ref} and \mathbf{b}_{ref} are replaced by the predicted (a priori) \mathbf{q} and \mathbf{b} after time update. Although STT and VSGA data are obtained at periods of 4 and 10 Hz, respectively, time and measurement updates are conducted at a period of 1 Hz, which corresponds to the ACS control period.

3. Preflight Test for the SDS-4 Attitude Determination System

Attitude Control Flight Software (ACFS) was evaluated through a full-software simulation test and a hardware-in-the-loop simulation test. As in the end-to-end evaluation of the attitude determination system, real sky tests using the PFM of SDS-4 spacecraft were conducted to confirm its function, and full-software simulation tests were implemented to evaluate its performance.

3.1. Real Sky Tests using the SDS-4 PFM

The real sky tests using the SDS-4 PFM are very unique and take advantage of micro satellites. The SDS-4 PFM was located outdoors and implemented dynamic attitude determination using STT, VSGA, DSS and MAGS. Through these tests, we could confirm the end-to-end function of the attitude determination system, including verification of its polarity. The relatively small ground system allowed such venturesome tests. Figure 7 shows the pictures taken during these tests, left and right for tests using STT and the QUEST method, respectively. The satellite was protected from outside contamination by a clear plastic container.



Figure 7. Real Sky Test using the SDS-4 PFM

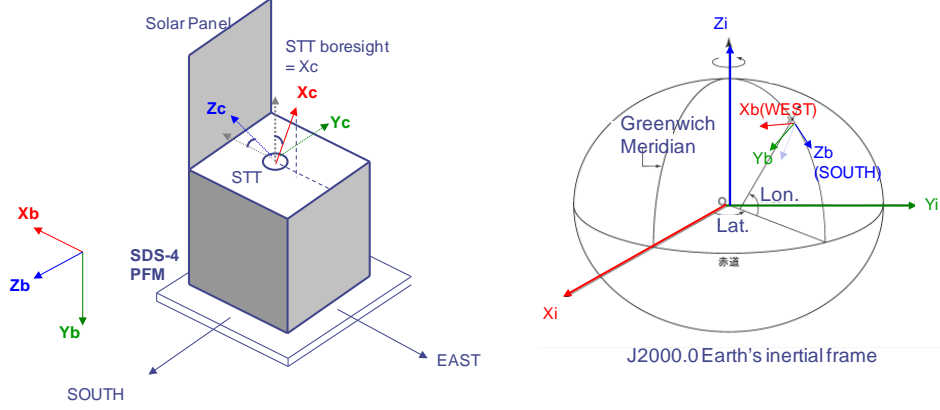


Figure 8. Schematic Diagram of the Test Configuration

Evaluation of attitude determination using STT was conducted in the real sky test at night. The SDS-4 PFM was located with STT boresight pointing at the sky. Figure 8 shows a schematic diagram of the test configuration. It is important that the satellite was located with its roll (X_b) axis pointing in the Earth's geographical westerly direction as precisely as possible, in which case the EKF estimated quaternion \mathbf{q}_{est} should have been approximately given by

$$\mathbf{q}_{est} = \text{dcm2quate}(\mathbf{C}_{eci2body}), \quad \mathbf{C}_{eci2body} = \begin{bmatrix} 1 & 0 & 0 \\ 0 & \cos \beta & \sin \beta \\ 0 & -\sin \beta & \cos \beta \end{bmatrix} \cdot \begin{bmatrix} \cos \alpha & \sin \alpha & 0 \\ -\sin \alpha & \cos \alpha & 0 \\ 0 & 0 & 1 \end{bmatrix} \quad (7)$$

$$\alpha = GST + Lon. - 90 \text{ [deg]}, \quad \beta = -180 + Lat. \text{ [deg]}$$

where $\mathbf{C}_{eci2body}$ represents the coordinate transformation matrix from the inertial frame to the satellite's body frame and 'dcm2quate()' means the process for conversion of a coordinate transformation matrix into a quaternion. GST, Lat. and Lon. indicate the Greenwich sidereal time, latitude and longitude of the satellite's location, respectively. We could examine the rough performance and confirm the end-to-end polarity according to this equation. In addition, we temporally covered the STT view with a cloth to see whether the EKF could derive the attitude quaternion without a measurement update. We also rotated the satellite at a velocity of about 3 deg/s to evaluate the continuous calculation of attitude quaternions and its rough accuracy.

Evaluation of attitude determination using the QUEST method was conducted in the real sky test during periods of sunlight similarly to the STT test mentioned above. The influence of the external environment on DSS and MAGS measurements, such as clouds, local magnetic fields, and so on, was measured beforehand and included into the evaluation.

3.2. Full-Software Simulation Test Results

The ACS attitude determination performance was evaluated through a software simulation test. Figure 9 indicates a typical three-axis attitude determination result during one orbital period. The graph on the right indicates the measurement error of the attitude calculated via the QUEST method, while the orange dotted line and violet thin line represent the presence of sunlight and validity of the QUEST attitude, respectively. During the preflight phase, we set a threshold for the valid angular range between the sun and magnetic field vectors of 45 – 135 deg, to avoid inaccurate measurement. Under such restriction, the measurement error of the QUEST attitude is

reduced to about 2.0 deg (3σ) in total axes. The graph on the left shows the eventual attitude determination error of EKF estimation. In the region where the pink line is up, STT measurement is used for measurement update. The green line represents the measurement update by the QUEST attitude. In the region where neither line is up, there is no measurement update and the satellite's attitude is solely estimated by gyro propagation. During the preflight phase, the availability of STT was assumed to be from the middle of the eclipse period to the middle of the sunlight period. Therefore, no measurement update was obtained during the former half of the eclipse period. There were also such regions with periods of sunlight, since we set a waiting time of 7 minutes before using the QUEST attitude as an alternative to STT, in addition to the threshold for the valid angular range in the QUEST method. The attitude determination error is 0.076 deg (3σ) in total axes in the region where STT is available, and 0.3 deg (3σ) when the QUEST attitude is used for measurement update. The error increases during gyro propagation and reaches 1.2 deg at times of eclipse.

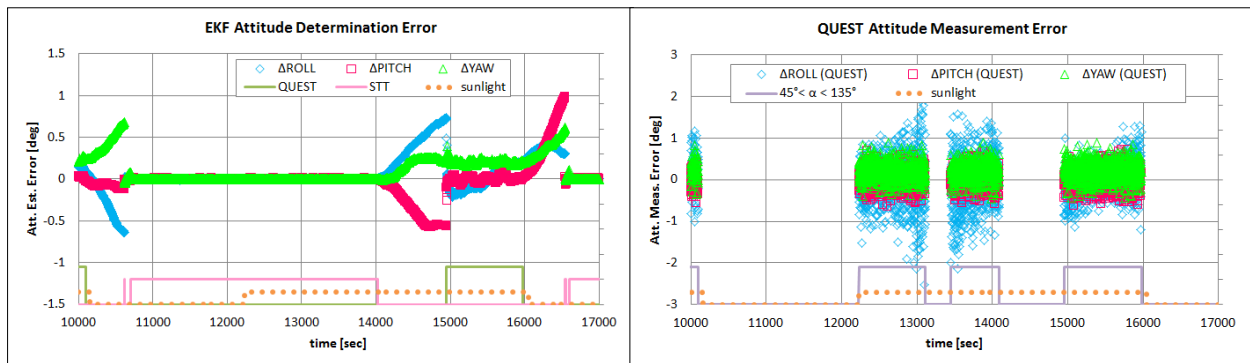


Figure 9. Attitude Determination Error in One Orbital Period

4. Flight Result

After the critical phase completed on 20 May, 2012, ACS started a three-axis control of the satellite. During the following commissioning phase, we conducted an initial check on the ACS components and confirmed the functions of attitude determination and control. Since then, we have been striving to improve the attitude determination performance. Although some unexpected behavior was observed and there was a slight difference from the predicted performance, SDS-4 is being operated successfully. Efforts for improvement, such as the calibration of the ACS components and tuning of the EKF parameters, have shown beneficial effects. In this section, we report on the results of the attitude determination performance over the past 5 months of operation.

4.1. Availability of Star Tracker

STT availability is the key factor determining the performance of attitude determination. There has been a significant difference between actual in-orbit and predicted availabilities.

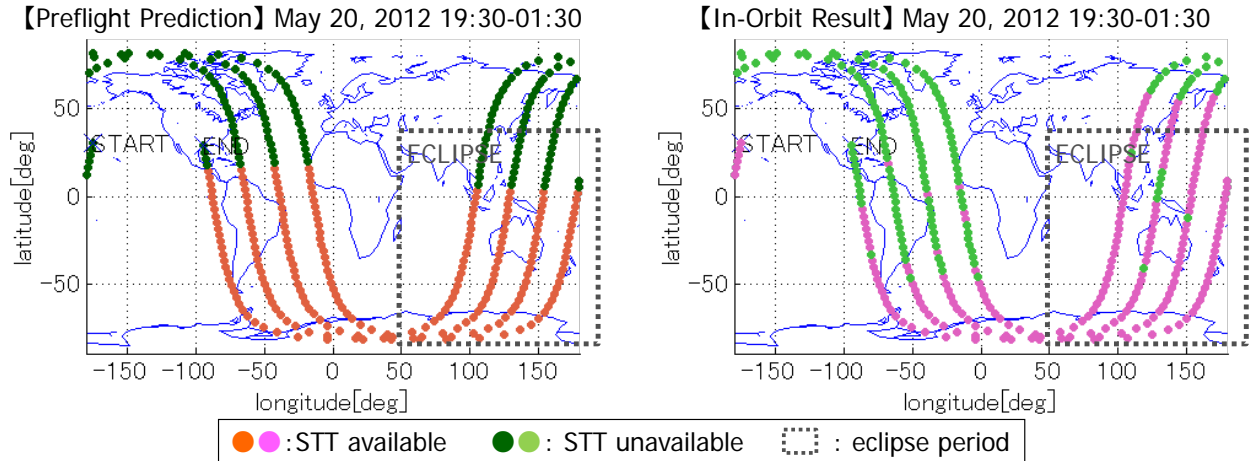


Figure 10. STT availability

Figure 10 shows the typical trend of STT availability which was predicted (left) and that actually obtained in orbit (right). The orange and pink dots indicate the regions where valid STT measurement is obtained. Unlike the preflight understanding, STT can provide attitude quaternions for almost all eclipse regions. In addition, it becomes available before entering the eclipse period. This situation is preferable, and suggests that STT can continue measurements when the Earth partially masks its field of view, and that the Earth exclusion angle of STT may be narrower. Conversely, STT is regularly unavailable for more than half the period of sunlight, which is likely attributable to its inappropriate layout. It seems the sunlight reflected from the Earth's surface is re-reflected by the back surface of the satellite's solar panel and enters the Earth exclusion angle, resulting in the unavailability of STT during periods of sunlight. Figure 11 shows the schematics of the STT layout, with the edge of the Earth exclusion angle crossing the solar panel. The right pictures in this figure was taken by the on-board monitor camera attached to the opposite side of STT, which indicates that the back surface of the solar panel is lightened by the reflected sunlight from the Earth's surface. It is noted that STT sometimes provides valid but inaccurate quaternions randomly during such regions, which increases the error rate for attitude determination.

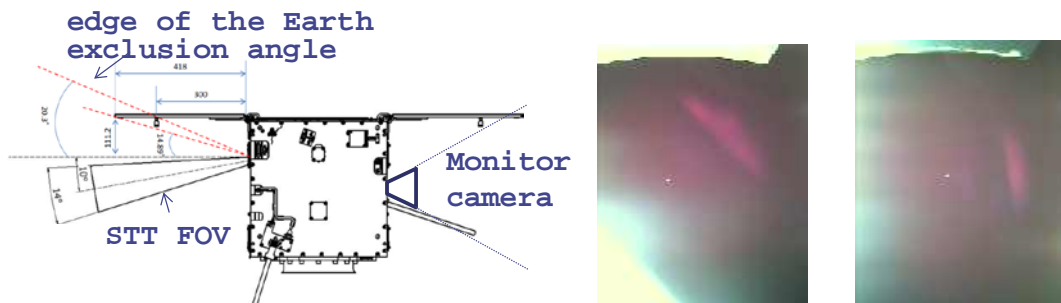


Figure 11. Layout of STT

4.2 Attitude Determination Error in the Early Operation

The top graph in Fig. 12 shows the sun angle detected by DSS during 3 orbital periods in the early operation. These data were obtained every 30 seconds. To avoid confusion, sun angle data

including the sunlight refraction effect, which is to be mentioned in chapter 5.2, are not plotted in this graph. Since DSS is attached with a boresight axis along the satellite’s roll axis, the sun angle can be assumed as approximately equivalent to pitch and yaw errors against the reference attitude. It is noted that this sun angle excludes the DSS error of 0.52 deg (3σ , random) and 0.064 deg (3σ , bias), which should be added to the error evaluation. The pink, orange, and green lines indicate the same flags as in Fig. 9. As mentioned above, the behavior of the pink line, namely, the availability of STT differs from the prediction. Compared with the prediction shown in Fig. 9, pitch and yaw errors during the availability of STT are relatively large. In addition, they exceed those obtained when the measurement update was conducted by the QUEST method. However, this is not important since they are assumed to be attributable to the error of DSS itself. The key aspect is the significance of error increase during gyro propagation in periods of sunlight, which peaks at about 2.0 deg. This is mainly attributable to the following two factors: longer propagation time due to unexpected STT unavailability and an inappropriate thermal calibration parameter for VSGA.

The bottom graph in Fig. 12 shows the error angles of the EKF determined attitude relative to the STT measurement. In this evaluation, STT measurement is assumed to be true. Note that there is no information in regions where STT measurement is unavailable. Although it is inappropriate to evaluate the attitude determination error by STT, we take it for a reference since there is no other sensor available to measure the satellite’s attitude more accurately. It must be noted that STT includes errors of 0.052 deg (3σ , random) and 0.081 deg (3σ , bias). The peaked increase in periods of sunlight without any change in measurement flags may be attributable to the inaccurate measurement of STT due to the stray sunlight in the Earth exclusion angle. As the arrows in this graph indicate, the gap generated when the STT measurement replaces the QUEST measurement is significant, particularly around the roll axis. This is assumed to be primarily attributable to the error in the QUEST measurement and shows the potential to improve by calibrating MAGS parameters and tuning the measurement noise covariance in EKF.

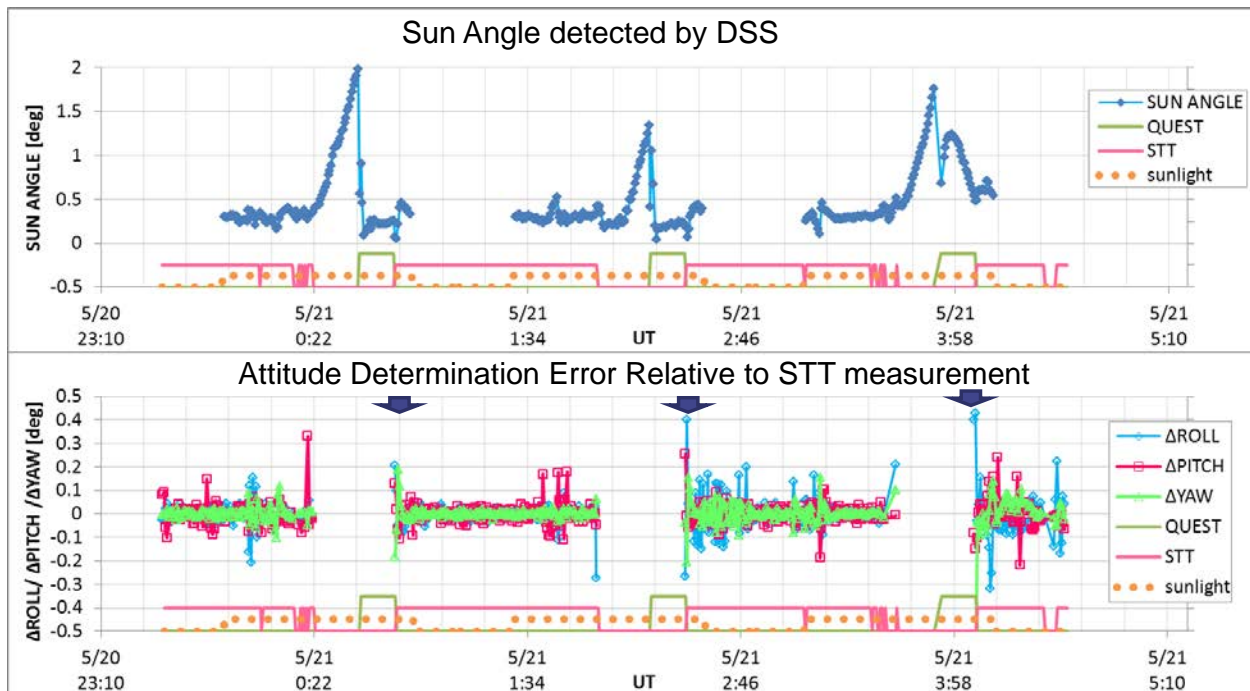


Figure 12. Attitude Determination Error in the Early Operation (3 orbital periods)

4.3. Attitude Determination Error After Efforts for improvement

To improve the attitude determination accuracy, we conducted efforts as follows: calibration of VSGA's thermal parameter, correction of misalignment in STT and DSS (as far as possible), calibration of MAGS's parameters, tuning of measurement noise covariance of STT and the QUEST, use of the QUEST attitude without restrictions such as the threshold for valid angular range and the waiting time as mentioned before. In particular, the calibration of VSGA and MAGS, and the use of the QUEST attitude for larger time periods have been effective. It was found that measurement updates with QUEST attitude enhance accuracy more than single gyro propagation, even during periods when the angle between the sun and magnetic field vector becomes parallel, since the EKF can properly cope with such errors. Figure 13 indicates the result during one orbital period after these efforts. The format of these graphs is the same as Fig. 12 and their data were obtained every 5 seconds.

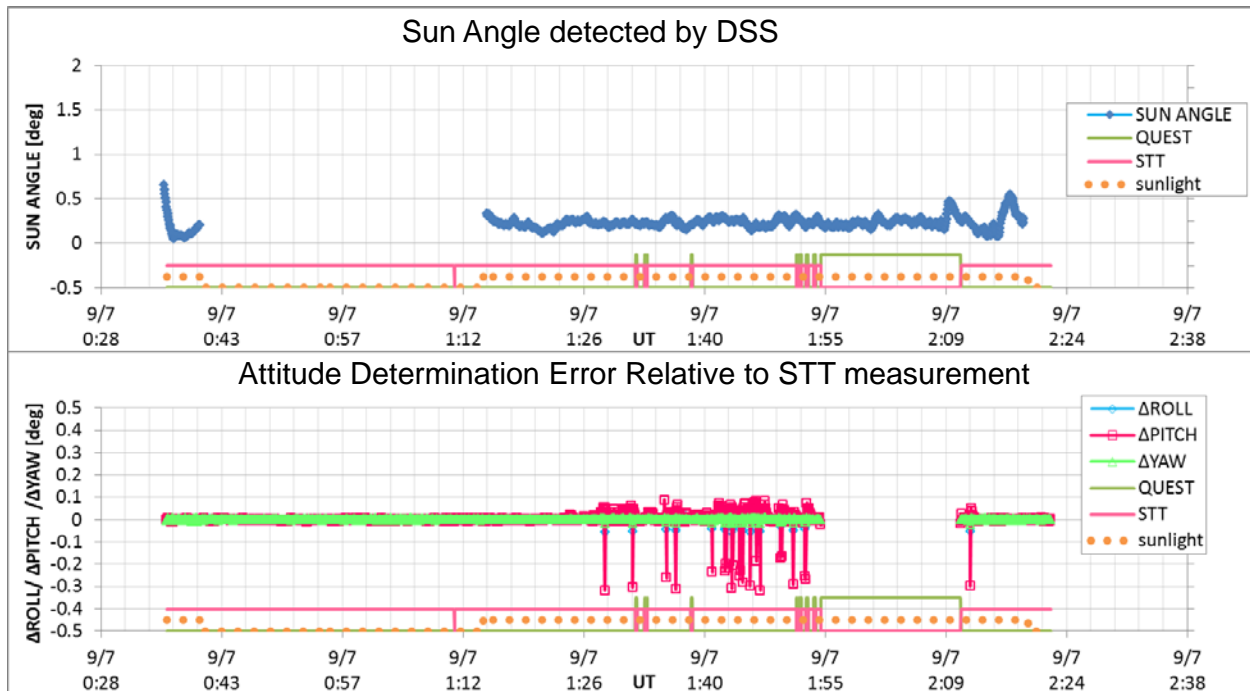


Figure 13. Attitude Determination Error After Operation for Improvement

Although the bottom graph shows some sudden increases in sunlight time due to inaccurate STT measurement, these graphs show how accuracy has improved.

We think that there still remains further potential for improvement. Enlarging the measurement noise covariance for STT has a possibility to improve accuracy, which may make the attitude estimation less sensitive to such inaccurate STT measurement. Figure 14 shows the obtained results when we set the measurement noise covariance matrix, \mathbf{R} , to $10\mathbf{R}$ and $100\mathbf{R}$. Unfortunately, there has been seen little effect this time. Further consideration will be needed.

Currently, we assume an attitude determination accuracy of below 0.08 deg, according to the evaluation by STT measurement, including the possible random errors of STT. Although it is

difficult to discuss the accuracy during STT unavailability, the EKF error covariance could provide a reference, which indicates 0.61 deg (3σ) at a maximum around the roll axis. Table 2 lists the summary of the attitude determination error.

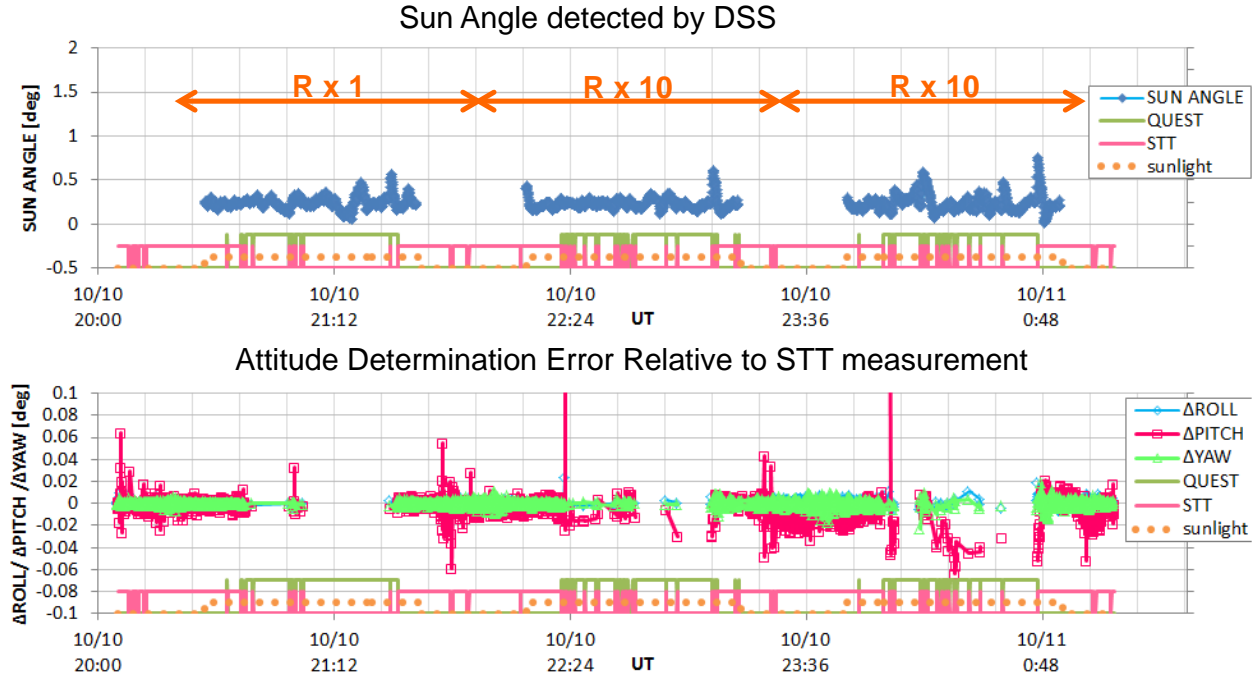


Figure 14. Attitude Determination Error at R = 1R, 10R, and 100R

Table 2. Attitude Determination Error Summary

Case		Roll Error [deg] (3σ)	Pitch Error [deg] (3σ)	Yaw Error [deg] (3σ)	Total [deg] (3σ)
Preflight Simulation	STT available	0.036	0.063	0.021	0.076
	STT unavailable	-	-	-	1.2 (worst)
In-orbit Results	STT available*1	< 0.028	< 0.070	< 0.026	< 0.080
	STT unavailable*2	0.61	0.078	0.078	0.62

*1: STT random error (0.052 deg in total axes, 3σ) is added.

*2: The EKF estimation error covariance is used as references.

5. Unexpected Behavior in Attitude Determination

In this section, we introduce some unexpected events occurred in orbit, which provided us useful knowledge.

5.1. Large Estimation Error in Gyro Rate Bias due to the EKF Reset

SDS-4 ACS has a function to reset the EKF attitude estimation. Here, ‘reset’ means initializing the predicted (a priori) estimate covariance \mathbf{P} - into a big number. When the difference between predicted (a priori) and measured quaternions, $\Delta\mathbf{y}$, exceeds the predetermined threshold, \mathbf{P} - is automatically initialized. This function is included for avoiding EKF divergence in the event of any anomaly. At the first stage, we set the threshold to 5 deg, which corresponds approximately

to the 3σ value of preflight-estimated error in the QUEST measurement. However, the EKF reset occurred far more frequently than expected, sometimes resulting in severe situations. This was attributable to the following three factors: anomalous behavior of STT, inappropriate threshold setting, and larger error in MAGS measurement. As mentioned above, STT measurement becomes unavailable for some time during periods of sunlight. The problem is that, shortly before it becomes completely unavailable, STT randomly provides quaternions which contain significant errors. When such errors exceed the threshold level, the EKF reset occurs. In addition, since the error in MAGS measurement was larger in orbit before calibration than that measured in the ground test, the calculated attitude via the QUEST method also had significant errors, which sometimes exceed the threshold. A severe situation occurs when such error output persists after the EKF reset, resulting in a significant error in estimating gyro rate bias. The graph in Fig. 15 shows the change in Kalman gain over time. When the EKF reset occurs, the Kalman gain which contributes to rate bias estimation is set to -2.0, and then gradually increases, taking 30 seconds or more to converge. As shown in the equations in Fig. 15, the Kalman gain \mathbf{K} determines how much $\Delta\mathbf{y}$ is assumed for the updated estimation error $\Delta\mathbf{b}$. If anomalous measurement continues and $\Delta\mathbf{y}$ remains large after the EKF reset, the estimated rate bias \mathbf{b} becomes much larger than its true state. If measurement update stops at this point, attitude propagation must start with such significant bias errors, which eventually result in a loss of satellite attitude.

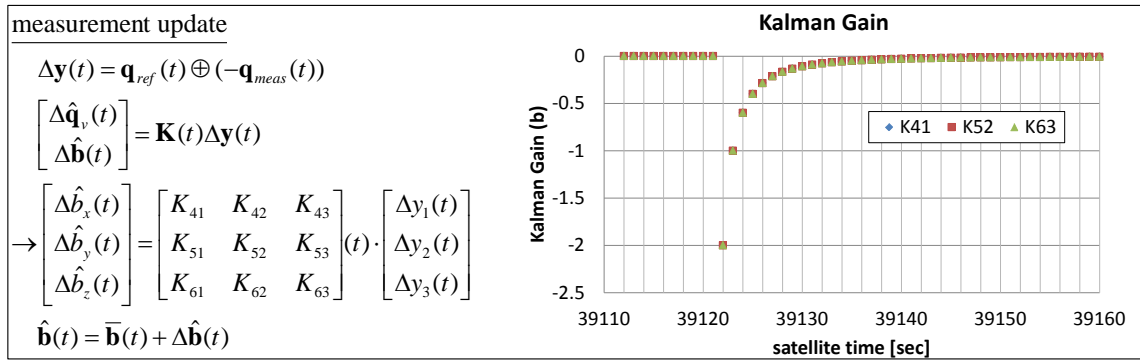


Figure 15. Kalman Gain after the EKF reset

Figure 16 shows the in-orbit satellite's behavior when such situation occurred. The graphs indicate from top to bottom, the controlled angles which ACS recognizes as an error relative to the reference attitude, the sun angle detected by DSS, including the measurement update and sunlight flags, and the on-board estimated rate biases. As shown in the top and middle graphs, during the satellite time from 1039000 to 1040000, the sun angle oscillated around 40 deg, though ACS thought there was little error to be controlled. The bottom graph shows that the on-board estimated rate bias reached 3.0 deg/s during this period, which is inconceivable and very likely to have caused this situation. Unfortunately, we cannot specify where and by what the EKF reset was caused, since these data were obtained at 1-minute intervals. However, it can be assumed that an anomalous STT output caused an EKF reset around the time where the left arrow in the middle graph points, and no measurement update was conducted afterward until normal STT measurements were obtained for a few seconds around the time period where the right arrow points. Although the QUEST attitude estimation was conducted in periods of sunlight, they were not applied to measurement updates as an alternative to STT. This is because, in the

early operation phase, we set a threshold for the valid angular range between the sun and magnetic field vectors, and a waiting time of 7 minutes before using the QUEST attitude as an alternative. After this event, the threshold for the EKF reset was updated with a sufficient margin, considering the anomalous STT output and the measurement error of MAGS. Additionally, in preparation for further anomaly in STT, which possibly causes such situations again, we examined the threshold settings for the QUEST measurement with a number of experimental operations and concluded that no restriction is preferable. This result also contributed to the improvement in the attitude determination accuracy.

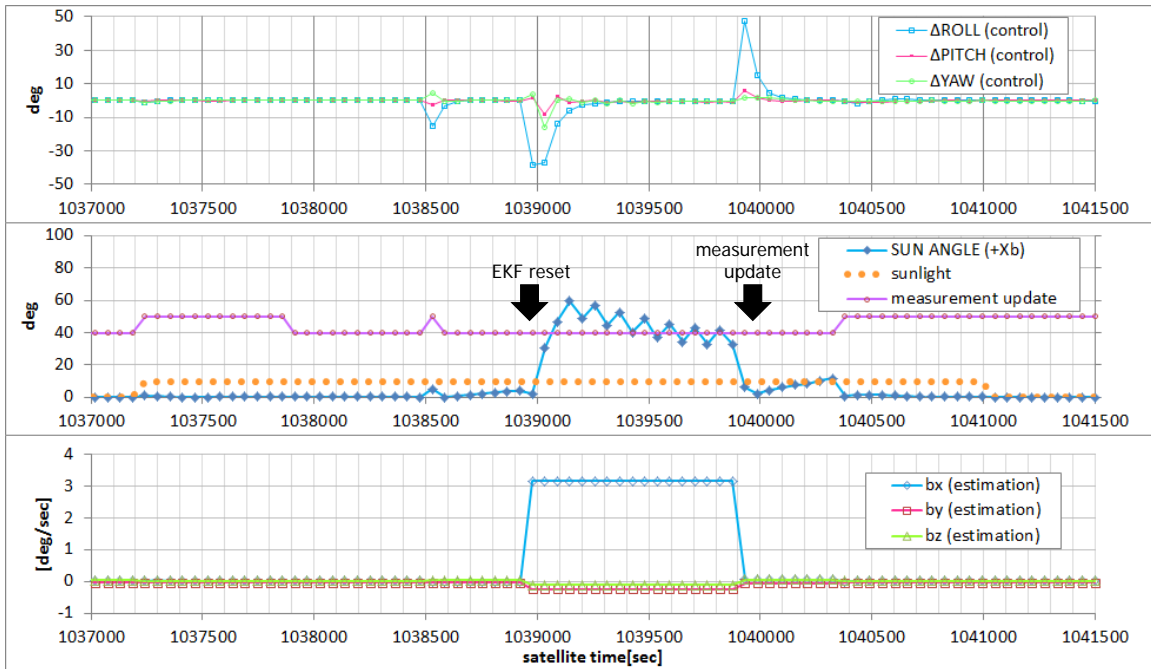


Figure 16. Unexpected Loss of Attitude due to the EKF Reset

5.2. Sunlight Refraction Effect on Gyro Rate Bias Estimation

Since DSS is attached to the same surface as the solar panels, the sun angle detected by DSS ought to be zero when the three-axis control is successfully conducted. However, as shown in the left graph in Fig. 17, the sun angle data always indicates a steep increase, reaching about 1.5 deg when the satellite is entering or exiting an eclipse. This can be explained by the refraction of sunlight in the Earth’s atmosphere. The right sketch in Fig. 17 shows a conceptual diagram of the sunlight refraction effect. Since the measurement update is conducted with STT during those periods, as indicated by the pink line in the graph, the attitude determination is unaffected by sunlight refraction and the satellite is controlled inertially-fixed. However, for the QUEST attitude determination, the sunlight refraction applied a certain error, since the QUEST method uses the sun vector detected by DSS. According to the in-orbit experiment in which the QUEST attitude is used to update measurement during those periods, the generated errors in the EKF estimation of satellite’s attitude and gyro bias rate reached about 0.06 deg and 0.001 deg/s, respectively. To reduce such errors, tuning of the measurement noise covariance and inhibiting the use of the QUEST attitude during those periods were found to be effective through experimental operations.

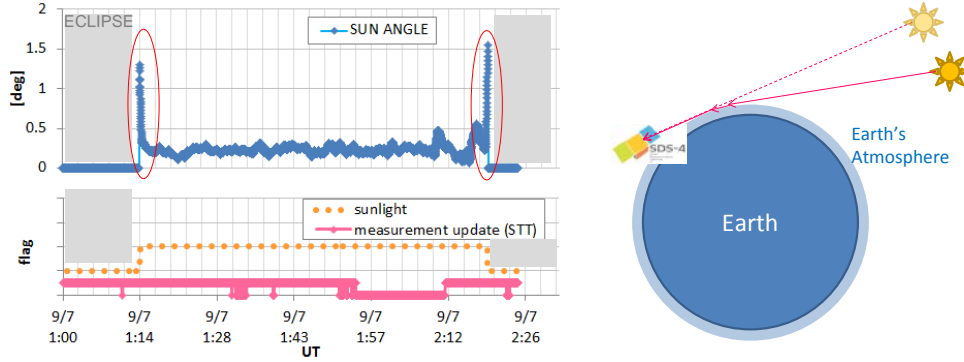


Figure 17. Sunlight Refraction Effect

5.3. Oscillatory Response in the Satellite’s Angular Rate

Although the following event was found to have no direct relationship with the attitude determination, we introduce it as an interesting case: Small oscillatory responses in the satellite angular rate were occasionally observed in orbit. The rotation speed data of RWs also showed the same responses during these periods. Figure 18 indicates the angular rate of the satellite and the rotation speed of RW under such events.

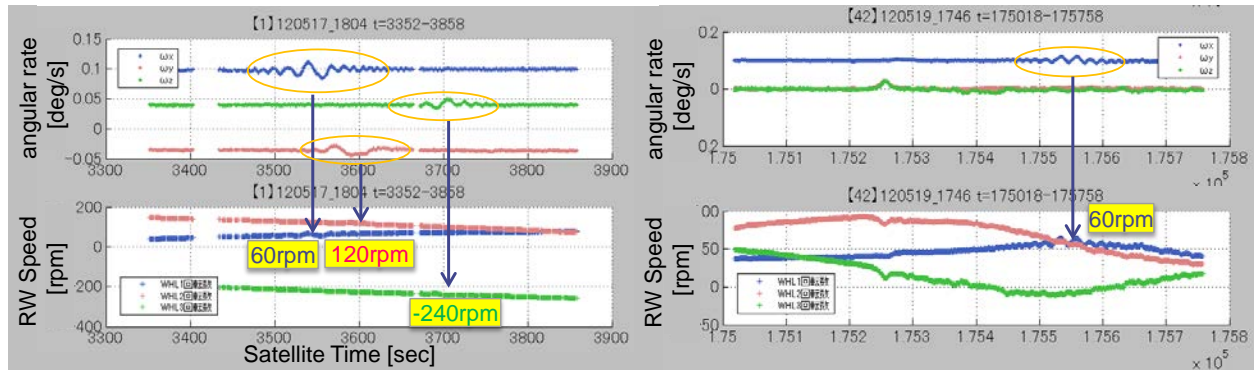


Figure 18. Oscillatory Response in Satellite’s angular rate and RW Rotation Speed

The responses appeared and faded without any particular trigger, and occurred even before three-axis control was started. After a month of investigation, it was found that these responses were likely to be caused by the aliasing effect between the ACS controller sampling and the nearly sinusoidal noise on the rotation speed telemetry of RWs. The RW of SDS-4 has a speed control loop and it is driven at a speed command from ACS. The ground test results showed that the rotation speed telemetry of RW has nearly sinusoidal noise whose frequency $f_{RWnoise}$ ranges from 0 to 2.5 Hz, depending on its rotation speed, as shown in Fig. 19. When ACS samples the telemetry data at the ACS control frequency f_{ACS} of 1Hz, the observed RW speed fluctuates at a frequency of $f = f_{ACS} - f_{RWnoise}$ due to an aliasing effect. If it reaches to the ACS control bandwidth of $\omega_c = 0.006 - 0.008$ Hz, that is to say, the noise frequency $f_{RWnoise}$ comes close to 1 or 2 Hz, ACS controller responds to this fluctuation and the satellite begins to show the oscillatory response. Figure 18 shows that the oscillation occurs when the RW speed is about 60, 120 and -240 rpm, in which the frequency of the sinusoidal noise is about 1, 2 and 1 Hz,

respectively, according to Fig. 19. It is noted that the amplitudes of these responses are negligible and such responses are certain to fade according to the change in the RW speed.

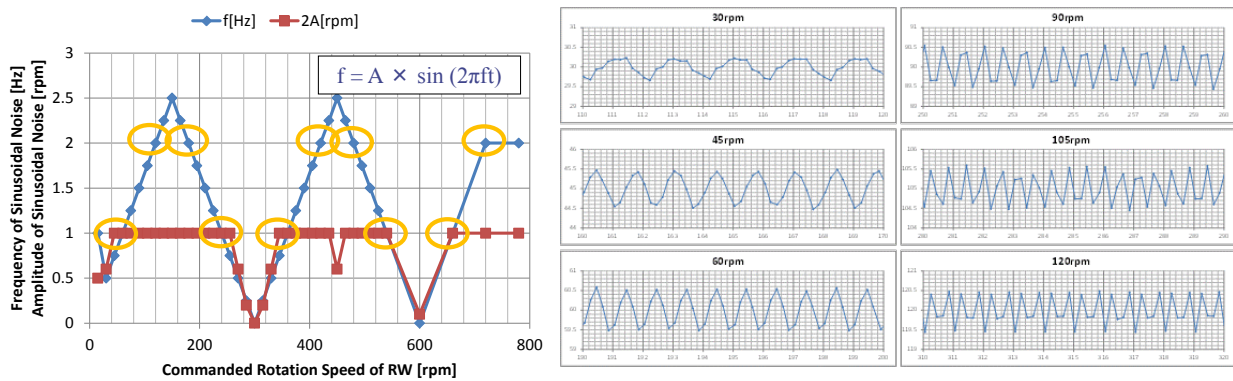


Figure 19. Sinusoidal Noise on the RW Rotation Speed

6. Conclusion

SDS-4, the first zero momentum three-axis controlled 50 kg-class piggyback satellite in Japan, was launched in May 2012 and is now operating effectively. Although certain unexpected behavior occurred, several efforts to improve the on-board attitude determination accuracy have been made and are now delivering beneficial effects over its 5 months of operation. Approaches for further improvement are ongoing.

7. Acknowledgements

This work received considerable support from other staff members inside the SDS-4 project team. The authors would like to acknowledge in particular the testing support provided by Mr. Fukuyama and Mr. Ogawa from Advanced Engineering Services CO., Ltd.

8. References

- [1] N. Murakami, Y. Nakajima, T. Ohtani, Y. Nakamura, K. Inoue, K. Hirako, “Preliminary Flight Result and Architecture of SDS-4 Attitude Control Subsystem”, IAC-12.C1.3.10, Proceedings of the 63rd International Astronautical Congress, Napoli, Italy, 2012.
- [2] Y. Nakajima, Y. Nakamura, H. Kawara, N. Murakami, T. Ohtani, K. Inoue, K. Hirako, “Development of a high Accuracy MEMS Rate Sensor for Small Satellites”, IAC-11-B4.6A.11, Proceedings of the 62nd International Astronautical Congress, Cape Town, South Africa, 2011.
- [3] Y. Nakajima, N. Murakami, T. Ohtani, Y. Nakamura, K. Inoue, K. Hirako, “SDS-4 Attitude Control System: First Flight Results of Attitude Control Response”, IAC-12.C1.9.3, Proceedings of the 63rd International Astronautical Congress, Napoli, Italy, 2012.
- [4] T. Ohtani, Y. Nakajima, Y. Takahashi, K. Inoue, K. Hirako, “First Flight Result of Japanese Technology Demonstration Mission SDS-4”, IAC-12.B4.6A.2, Proceedings of the 63rd International Astronautical Congress, Napoli, Italy, 2012.